

# Automatic resting-state fMRI Independent Component Classification using Support Vector Machines

Yanlu Wang<sup>1,3</sup> and Tie-Qiang Li<sup>1,2</sup>

<sup>1</sup>Clinical Science, Intervention, and Technology, Karolinska Institute, Stockholm, Stockholm, Sweden, <sup>2</sup>Medical Physics, Karolinska University Hospital, Huddinge, Stockholm, Sweden

**Target Audience:** Clinicians and neuroscientists who are interested in using independent component analysis (ICA) for resting-state fMRI (rs-fMRI) studies and MRI physicists who are interested tools to facilitate ICA-based analysis of rs-fMRI data.

**Purpose:** Independent component analysis (ICA) is a useful method to analyze and extract meaningful functional networks from rs-fMRI data. However, the output of independent components (ICs) is usually contaminated with various artifacts and must be manually evaluated, usually through visual inspection<sup>1</sup>. This process quickly becomes cumbersome with increased number of ICs. We propose an automated classification framework with two-fold purpose: 1) Automatically identify and separate ICs contaminated by noise and artifacts; 2) use the framework to study the ICA dimensionality of the resting-state fMRI data.

**Methods:** We performed a series of ICA on a set of rs-fMRI data from 20 to 100 output ICs. The dataset consists of a total of 26 healthy subjects (male/female=11/15, age=13-29) scanned using a Siemens Allegra 3T MRI scanner. Three rs-fMRI scans were performed for each subject with 197 dynamic timeframes of EPI volumes with 39 slices, TR/TE=2000/25ms; FoV=192mm; matrix size=64x64, and flip angle=90. Classifiers were devised based on “typical instructions for visual inspection”: Functional connectivity networks should exhibit peak activation in cortical grey-matter, and possess little spatial overlap with known vascular, ventricular, motion, and susceptibility artifacts<sup>2</sup>. The significant ( $p<0.01$ ) classifiers were used to train a model for our framework using the training set of 30 ICs, which were manually classified through visual inspection. The model was then used for our SVM classification framework to automatically classify all test sets from 20 to 100 ICs. Visual inspection for selective ICs sets (50, 70, and 90 ICs) was performed to evaluate the performance of the framework.

ICA was performed on a secondary set of rs-fMRI data with 30 output ICs and classified using the previously trained model. The dataset consists of a total of 86 normal subjects (male/female=40/46, age=21-84) scanned using a Siemens Trio 3T clinical MRI scanner. With a 32-channel phased array detector. A single-shot 3D-EPI was used with acquisition parameters: 32 transverse slices 3.6mm thick; TE/TE=200/35ms, FoV=220mm; IPAT=2; flip angle=90; matrix size=64x64, and 300 timeframes. This is to verify that our classification framework can be used independently of the training dataset.

**Results:** Based on the instructions for visual inspection, a total of 18 classifiers were devised, of which 5 were significant ( $p<0.01$ ) in their explanatory power. For the evaluated ICs sets (50, 70, and 90 ICs), prediction accuracy was on average 13% for false positive rates and 0% false negative rates in noise/artifact IC identification (Table 1). Prediction accuracy was 100% in true positive and true negative rates for classification of the secondary rs-fMRI dataset, showing that our framework will function across rs-fMRI datasets.

**Discussion:** Achieving 0% false negative rates for noise/artifact identification is essential for an automatic noise/artifact removal program. We achieved this through conservative labeling of noise/artifact ICs during visual inspection of the training ICs. Prediction accuracy achieved by our framework can be compared to the 94% overall true positive rates for BOLD signal classification by another SVM-based classification study<sup>3</sup>.

The misclassified ICs were examined for cause of misclassification (Fig. 1). The mislabeled ICs can be considered as borderline cases where the components depict resting-state networks that are also contaminated by artifacts. The ICs were labeled as artifacts during the visual inspection process based on to prior knowledge that these areas are prone to different types of artifacts such as susceptibility (Fig. 1-A), and motion (Fig. 1B, C). This information was not available to our framework and perhaps could be incorporated as masks for better prediction accuracy in the future.

**Conclusion:** Our framework is capable of removing the majority of noise/artifact ICs without misclassifying any potential resting-state functional connectivity networks. Automatic classification of ICs greatly facilitates ICA-based analysis of rs-fMRI data with high model orders.

## References:

- <sup>1</sup>Bartels A, Zeki S. (2005). Neuroimage 24(2): 339-349.
- <sup>2</sup>Cordes D, Nandy RR. (2006). Neuroimage 29(1): 145-154.
- <sup>3</sup>De Martino F, et al. (2007). Neuroimage 34(1): 177-194.

**Table 1: Prediction Accuracy for all evaluated ICs sets (50, 70, and 90).  $N_{TOT}$  is the total number of ICs in a set.  $N_{ART}$  and  $N_{RFN}$  is the total number of ICs identified as noise/artifact and resting-state networks respectively.**

| Dataset        | Prediction |           | True      |           |
|----------------|------------|-----------|-----------|-----------|
|                | $N_{TOT}$  | $N_{ART}$ | $N_{RFN}$ | $N_{ART}$ |
| 30             | 12         | 18        | 12        | 18        |
| 50             | 20         | 30        | 23        | 27        |
| 70             | 33         | 37        | 38        | 32        |
| 90             | 48         | 42        | 52        | 38        |
| 30 (secondary) | 11         | 19        | 11        | 19        |

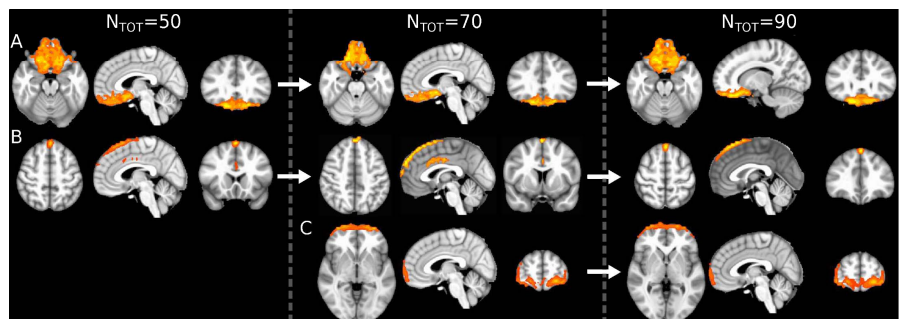


**Figure 1: All Misclassified ICs from evaluated test ICs sets. Some ICs are reoccurring through increased model orders and consistently misclassified.**